NANO
LETTERS

2009
Vol. 9, No. 9
3282-3289

Do Inner Shells of Double-Walled Carbon Nanotubes Fluoresce?

**Dmitri A. Tsyboulski,[†,¶] Ye Hou,[‡,¶] Nikta Fakhri,[§] Saunab Ghosh,[†] Ru Zhang,[⊥]
Sergei M. Bachilo,[†] Matteo Pasquali,[†,§] Liwei Chen,[*,#] Jie Liu,[*,‡]
and R. Bruce Weisman[*,†]**

Department of Chemistry and R.E. Smalley Institute for Nanoscale Science and Technology, Rice University, 6100 Main Street, Houston, Texas 77005, Department of Chemistry, Duke University, Durham, North Carolina, 27708, Department of Chemical and Biomolecular Engineering and Center for Biological and Environmental Nanotechnology, Rice University, Houston, Texas 77005, and Department of Physics and Astronomy, Department of Chemistry and Biochemistry, Ohio University, Athens, Ohio 45701

Received May 14, 2009; Revised Manuscript Received July 8, 2009

ABSTRACT

The reported fluorescence from inner shells of double-walled carbon nanotubes (DWCNTs) is an intriguing and potentially useful property. A combination of bulk and single-molecule methods was used to study the spectroscopy, chemical quenching, mechanical rigidity, abundance, density, and TEM images of the near-IR emitters in DWCNT samples. DWCNT inner shell fluorescence is found to be weaker than SWCNT fluorescence by a factor of at least 10 000. Observable near-IR emission from DWCNT samples is attributed to SWCNT impurities.

Double-walled carbon nanotubes (DWCNTs) are unusual artificial nanomaterials that are structurally intermediate between single-walled and multiwalled nanotubes (SWCNTs and MWCNTs).[1] In these structures, two SWCNTs are concentrically nested with typical interwall separations of approximately 0.37 ± 0.04 nm.[1−4] DWCNTs can be prepared directly in nanotube growth reactors,[3,5] or indirectly by thermal annealing of SWCNTs that have been internally loaded with fullerene molecules to form "peapods".[2] DWCNT samples produced by either production method contain some residual SWCNTs that are typically removed through thermal oxidation and acid treatment to achieve purity levels above 90%.[6,7] Even when such purification treatments do not totally eliminate SWCNT impurities, they are expected to quench effectively the characteristic near-IR fluorescence of residual SWCNTs,[8] because minimal sidewall chemical derivatization (∼1 per 10 000 C atoms) can significantly suppress SWCNT fluorescence.[9,10] Several groups have reported that aqueous suspensions of chemically purified DWCNT samples show considerable near-IR emission at wavelengths consistent with fluorescence from DWCNT inner shells.[7,11−15] High-resolution transmission electron microscopy (HRTEM) further confirmed a match between the diameter distributions of the inner shells of those DWCNTs and diameters of emitting nanotube species deduced from spectral analysis.[7,11] These experiments along with additional observations have led several investigators to conclude that inner shells of double-walled nanotubes fluoresce intensely in the near-IR.[7,11−17] By contrast, a study of DWCNTs synthesized through peapod annealing found severe quenching of inner shell fluorescence.[18] It was suggested that this quenching results from stronger intershell electronic coupling related to slightly smaller interwall spacings (<0.346 nm) in peapod-derived samples.[18] A recent study of CVD-grown DWCNTs purified by density gradient centrifugation found apparent inner shell fluorescence that was susceptible to acid quenching and approximately 6 times weaker than SWCNT fluorescence.[19] It was accordingly assigned to SWCNT impurities. DWCNT inner shell emission thus remains controversial.

In view of the well-known fluorescence quenching in nanotube bundles, which have intertube spacings of ∼0.32 nm,[21,22] and measurements showing efficient exoergic energy transfer from smaller to larger diameter SWCNTs separated by more than 1 nm,[20] one would expect inner shell emission to be severely quenched in all DWCNTs. Until fluorescence

---

[*] To whom correspondence should be addressed. E-mail: (R.B.W.) weisman@rice.edu; (L.C.) lwchen2000@gmail.com; (J.L.) j.liu@duke.edu.

[†] Department of Chemistry and R.E. Smalley Institute for Nanoscale Science and Technology, Rice University.

[‡] Duke University.

[§] Department of Chemical and Biomolecular Engineering and Center for Biological and Environmental Nanotechnology, Rice University.

[⊥] Department of Physics and Astronomy, Ohio University.

[#] Department of Chemistry and Biochemistry, Ohio University. Present address: Suzhou Institute of NanoTech and NanoBionics, Suzhou, P. R. China.

[¶] These authors contributed equally to this work.

10.1021/nl901550r CCC: $40.75

from samples of catalytically produced DWCNTs is unambiguously traced to inner shells, one should consider the possibility that the emission may come from fluorescent SWCNT impurities remaining after chemical purification. As such purification is typically performed on dry nanotube samples containing large aggregates,[7,11−13,15] one can imagine that residual SWCNTs inside aggregates might be shielded from chemical damage and then act as emissive impurities after being released during subsequent dispersion.

In an attempt to clarify the nature of DWCNT inner tube fluorescence, we prepared samples of purified CVD-grown DWCNTs. We then performed a set of bulk and single-particle measurements designed to reveal whether the emission was intrinsic to the DWCNTs in the sample, or instead arose from SWCNT impurities. We measured the single-emitter brightness, spectra, abundance, mechanical stiffness, chemical quenchability, and buoyant densities of emitting species in the samples. Our results clearly indicate that residual SWCNTs are the source of observable near-IR fluorescence commonly attributed to inner shells of DWCNTs.

DWCNTs were synthesized at Duke University by carbon monoxide chemical vapor deposition (CO−CVD) using a binary Co/Mo catalyst supported on MgO powder. The nanotube product was oxidized at 525 °C in Ar containing 20% air for 1 h and then refluxed in 3 N HCl solution to remove residual SWNCTs and obtain initial DWCNT purities estimated at ~95% from TEM imaging (see Supporting Information). As a SWCNT reference, we used raw nanotubes grown by the HiPco process (Rice University batch 162.8).

Suspensions were prepared by placing ~0.1−1.0 mg of solid nanotube material in 2 mL of aqueous 2% sodium deoxycholate (NaDOC) solution and sonicating the mixture for 2 h with a tip sonicator (Misonix XL-2000) at 8 W input power. During sonication, the sample temperature was stabilized with an external ice bath. Dispersions were mildly centrifuged for 30 min at 10 000 × g to remove large nanotube bundles. This centrifugation step was omitted for density gradient separation experiments. To prepare samples containing higher abundances of long (>3 μm) individual CNTs, we used milder dispersion conditions in which several micrograms of CNTs in 2 mL of aqueous surfactant solution were exposed either to 30 min of bath sonication (Fisher Scientific FS 14) or to intense but brief tip sonication (input power of ~ 5 − 7 W for 5 s).[23,24] Our methodology and apparatus for capturing images and spectra of freely moving or immobilized individual nanotubes have been presented in prior publications.[10,23,24] The procedure for measuring intrinsic fluorescence action cross sections of SWCNTs (the products of absorption cross-section σ and fluorescence quantum yield Φ_{FL}), has also been previously described.[24]

We investigated the susceptibility of DWCNT sample fluorescence to chemical derivatization by exposing suspended nanotubes to solutions of aryl diazonium salts known to react with nanotube sidewalls.[25] The 4-bromobenzenediazonium tetrafluoroborate reactant (Fisher Scientific) was used without further purification to prepare an aqueous 1 mg/mL solution. Near-IR fluorescence micrographs of individual nanotubes immobilized in agarose gel were then recorded while ~10 μL of this diazonium salt solution was deposited at the open edge of the sample slide and allowed to diffuse through the gel. We studied fluorescence quenching in bulk samples by adding 5 μL aliquots of the 4-bromobenzenediazonium tetrafluoroborate solution to 1 mL of nanotube suspension in a model NS1 NanoSpectralyzer (Applied NanoFluorescence, LLC).

Persistence lengths of individual long nanotubes present in weakly sonicated DWCNT suspensions were deduced from their bending amplitudes, as observed in near-IR fluorescence videomicroscopy using 659 nm laser excitation (0.2 to 1 kW/cm^2 intensity), 90× magnification, and a 50 ms frame acquisition time. The (n,m) identities of individual emissive nanotubes were deduced from their emission spectra.[26] As described in detail elsewhere,[27,28] the bending analysis began with finding each nanotube's backbone shape from near-IR images through a custom procedure based on an intensity-weighted center of mass method. The shape was then decomposed into Fourier modes according to the method of Gittes et al.[29] using the relation $\theta(s) = (2/L)^{1/2} \cdot \sum_{n=0}^{\infty} a_n \cos((n\pi s)/L)$. Here $\theta(s)$ is the angle tangent to the nanotube at contour position s, L is the total nanotube length, n is the mode number, and a_n is the mode amplitude. The amplitude of each mode was extracted by inverse Fourier transformation of this equation. At thermal equilibrium, the nanotube bending stiffness, χ, is found from the following inverse proportionality to variance of bending mode amplitude: $\chi = (k_B T/\langle a_n^2 \rangle) \cdot (L^2/(n\pi)^2)$. Here k_B is the Boltzmann constant, T is the ambient temperature, and angular brackets denote an ensemble average.

Fractionation of DWCNT samples was performed using an iodine-based density gradient medium (OptiPrep, a 60 wt % iodixanol/water mixture). Density gradients were formed in a 14 mm diameter ultracentrifuge tube by layering 715 μL volumes of premixed iodixanol/2% aqueous NaDOC solutions having iodixanol contents ranging from 7.5 to 35% in 2.5% steps. The tube was then held at an angle of ~10 degrees from horizontal for 1 h to allow diffusional formation of a linear density gradient. Undiluted OptiPrep was added to the DWCNT sample to raise its density to 1.173 g/cm^3 (32.5% iodixanol content). Then 1.5 mL of this sample solution was injected into the section of the centrifuge tube of similar density. The remaining volume in the tube was filled with a 2% NaDOC aqueous solution to within ~3 mm from the top. Samples were centrifuged for 16 h at 288 000 × g on a Sorvall Discovery 100 SE centrifuge equipped with a Beckman SW41-Ti rotor. After centrifugation, the sample was separated into ~280 μL fractions using a Biocomp 152 piston gradient fractionator.

We prepared samples for TEM analysis by mixing the suspended DWCNTs with ethanol using bath sonication, dropping the resulting solution onto a Cu grid coated with a lacey carbon film, and air-drying the sample. HRTEM imaging was performed using a Hitachi HF2000 microscope operating at an accelerating voltage of 200 kV.

Following conventional ultrasonic dispersion and centrifugation in aqueous surfactants, the DWCNT samples showed weak but clear near-IR fluorescence in the 950−1200 nm region characteristic of small diameter SWCNTs.[8,26] Photoluminescence maps revealed diameter distributions consistent with the inner shell diameters measured for the samples by high resolution transmission electron microscopy (HRTEM) (see Supporting Information). Careful examination showed that the emission peak positions were red shifted from those of pristine SWCNTs by ~1 to 4 nm, consistent with earlier observations.[11,15,17] Because the optical resonances of SWCNTs are somewhat sensitive to environment and chemical history,[30−33] it was unclear whether this shifted emission arose from DWCNT inner shells inside the special dielectric environment of their outer shells,[11,15,17] or instead from residual SWCNTs spectrally perturbed by sample processing.[33] To investigate this point, we compared emission spectra of pristine SWCNTs and SWCNTs that had been subjected to a milder form of the same purification procedures used for the DWCNT samples. We found that purification-processed SWCNTs showed similar emission red shifts of 1−5 nm relative to those of pristine SWCNTs (see Supporting Information). We therefore infer that the small red shifts in E_{11} fluorescence from chemically purified DWCNT samples do not provide secure evidence of inner shell emission.

If a DWCNT inner shell is electronically perturbed by the adjacent outer shell, it should show a different emissive quantum yield than a SWCNT of the same structure. Changes in spectral line width, reflecting environmental effects on exciton dynamics,[34,35] should also be evident when comparing DWCNT inner shells to equivalent SWCNTs. Measurements of fluorescence emission efficiencies and line widths may thus be useful in distinguishing SWCNT from DWCNT emitters. We first prepared SWCNT and DWCNT dispersions that were matched in surfactant, preparation method, and absorbance. As illustrated in Figure 1a, the DWCNT bulk suspensions showed near-IR emission that was significantly weaker, by a factor of ~5 in the case shown. However, it is difficult to draw definitive conclusions from comparative measurements on bulk samples because of possible differences in (*n*,*m*) distributions, unknown (*n*,*m*)-dependent molar absorptivities, overlapping absorption features, and uncertain contents of bundles and impurities.

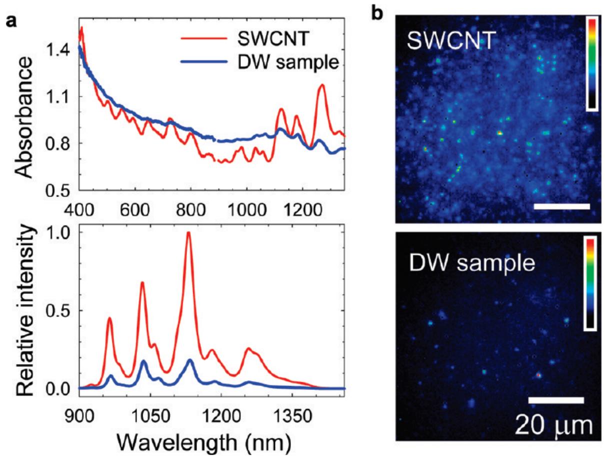

Figure 1. Optical properties of individual near-IR emitters in SWCNT and DWCNT suspensions. (a) Comparative absorption and emission spectra of SWCNT and DWCNT samples suspended in 2% NaDOC/H_2O. The two samples were adjusted for similar absorbance values. (b) Near-IR fluorescence images of these suspensions, recorded under the same experimental conditions (excitation wavelength 659 nm, excitation intensity ~800 W/cm^2, frame acquisition time 50 ms) and displayed on the same false-color intensity scale.

A much more direct approach is to use near-IR fluorescence microscopy to measure the relative emissive brightness of individual nanotubes in the samples. Figure 1b shows typical near-IR fluorescence images of these suspensions recorded under identical experimental conditions and displayed on the same intensity scale.[23] It appears that the DWCNT sample contains a low concentration of emitters that are individually similar in brightness to those in the SWCNT sample. Quantifying the brightness of an individual nanotube requires care, however, because emission intensity will depend not only on quantum yield, but also on the nanotube length, its orientation relative to the excitation beam polarization, its (*n*,*m*) identity, and the difference between its E_{22} absorption peak and the excitation wavelength.[24] To control for these variables, we restricted observations to nanotubes that had optically resolvable lengths (greater than 2 μm) and could be identified from their emission spectra as (8,3), (7,5), or (7,6). These species have E_{22} peaks close to our 659 nm excitation wavelength. Figure 2a displays overlaid normalized emission spectra from individual (7,5) emitters in DWCNT and SWCNT samples, and the inset shows the near-IR fluorescence images of those nanotubes on a matched intensity scale. The two nanotubes are nearly identical in spectrum and emissive brightness per unit length. Figure 2b displays measured (7,5) line widths (full-width at half-maximum) and peak wavelengths for 8 SWCNTs and 12 emitters from a DWCNT sample. The data reveal no systematic differences between the samples in line widths, peak wavelengths, or their correlations. Using calibrated conditions for excitation and detection, we also measured their spectrally integrated emission signals per unit length. Figure 2c shows these fluorescence action cross sections for 14 SWCNTs and 16 emitters from the DWCNT sample. Note that the experimental values represent the product of fluorescence quantum yield and absorption cross-section per carbon atom at 659 nm (not at the E_{22} peak, as in our previous report[24]). Although the measured fluorescence action cross sections vary systematically with (*n*,*m*) species, no significant differences are seen between emitters from SWCNT and DWCNT samples. We thus find that individual fluorescent nanotubes of the same (*n*,*m*) species show equivalent emission peak wavelengths, emission line widths, and emissive brightness whether observed in SWCNT or in DWCNT samples.

Another approach to distinguishing SWCNT from DWCNT emission is to monitor fluorescence quenching caused by sidewall covalent functionalization. We have previously shown that exposure to diazonium salts causes

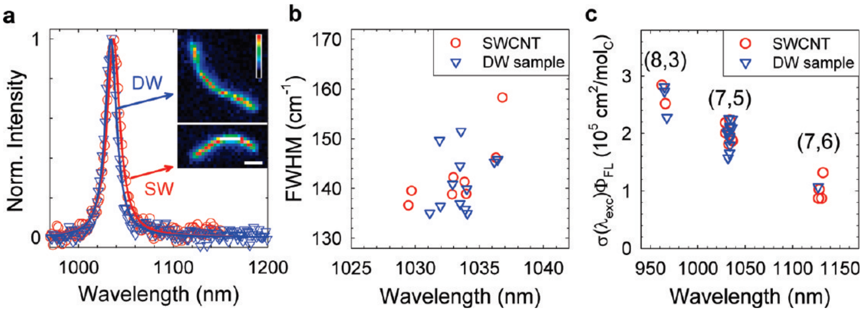

Figure 2. Spectral properties of individual near-IR emitters in SWCNT and DWCNT suspensions. (a) Examples of emission spectra and Lorentzian fits for "long" individual (7,5) nanotubes found in weakly sonicated SWCNT and DWCNT suspensions. Their fluorescence images are shown in the inset on the same false-color intensity scale. (b) Spectral linewidths (as full widths at half-maximum) of (7,5) nanotubes vs peak emission wavelength for 8 individual SWCNTs and 12 individual emitters in a DWCNT sample. (c) Fluorescence action cross sections vs emission wavelength for 14 SWCNTs and 16 individual emitters in a DWCNT sample. Clusters of data points are labeled with their (*n*,*m*) identities.

individual SWCNTs observed in near-IR fluorescence microscopy to display irreversible stepwise decreases in emission intensity reflecting single-molecule reactions with the nanotube.[10] It is expected that emission from a DWCNT inner shell would be far more resistant to such chemical quenching because the outer shell would protect against chemical attack. Indeed, there are indications that inner wall electronic structure remains intact while optical resonances of DWCNT outer shells are destroyed by covalent functionalization or electrochemical doping.[13,14] To ensure that the observed nanotubes were directly exposed to the functionalization reactant rather than trapped in the interior of nanotube bundles, we performed measurements only on well-dispersed samples.

We first monitored near-IR fluorescence from bulk DWCNT dispersions after adding aliquots of a diazonium salt solution known to functionalize carbon nanotubes.[36] Figure 3a shows emission spectra before and after two such additions. Fluorescence quenching was rapid and nearly complete for the more reactive large band gap species, as was observed in samples of SWCNTs.[37] We also studied this process by preparing immobilized DWCNT dispersions in agarose gels and then monitoring individual emitting centers using near-IR fluorescence microscopy. Each emissive object showed irreversible diazonium quenching. Figure 3b plots the emission intensity from two different segments of a long emissive nanotube in a DWCNT sample as a function of time after exposure to the diazonium solution. Emission from the DWCNT sample was quenched in locally stepwise patterns, and approximately 7 to 13 single-molecule reaction events were needed to quench 90% of the fluorescence from a 1 μm segment. These step sizes closely match those found earlier for SWCNTs,[10] implying that the exciton quenching efficiency of individual derivatization sites was not smaller for DWCNT emitters than for SWCNTs. We also observed that fluorescence from the DWCNT suspensions was readily quenched by exposure to acid or potassium permanganate (see Supporting Information). These results show that the chemical quenching behavior of DWCNT emitters is qualitatively and quantitatively similar to that of SWCNTs and indicate that the emitting centers in DWCNT and SWCNT samples have comparable exposure to the surrounding medium.

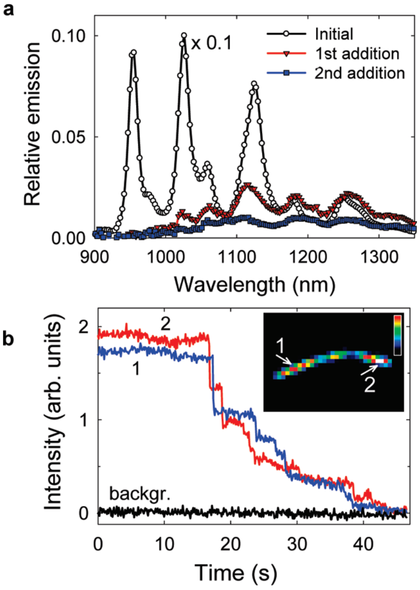

Figure 3. Fluorescence quenching of emitting species in a DWCNT sample by covalent functionalization. (a) Fluorescence spectra of a 1 mL DWCNT suspension after addition of 5 μL portions of bromobenzenediazonium salt solution. The initial spectrum has been scaled down by a factor of 10 for clarity. (b) Stepwise fluorescence quenching observed by plotting intensities from different segments of an immobilized individual long emitter in a DWCNT sample as a function of time after exposure to bromobenzenediazonium salt solution. The inset shows locations of the segments whose emission intensities are plotted in the main frame.

Another property that can be probed by near-IR fluorescence microscopy is the mechanical stiffness of emissive long nanotubes. In aqueous suspension, individual SWCNTs with lengths greater than 3 μm show noticeable bending induced by Brownian forces.[27,28,38] Mechanically, SWCNTs can be modeled as inextensible elastic beams with in-plane bending stiffness $\chi = EI$, where E is the elastic modulus and I is the area moment of inertia about the tube axis. The ratio of bending stiffness to thermal energy gives a characteristic persistence length $L_p = \chi/k_BT$.[39] L_p represents the length scale over which a nanotube shows significant curvature induced by thermal fluctuations. In a rcent experimental study of

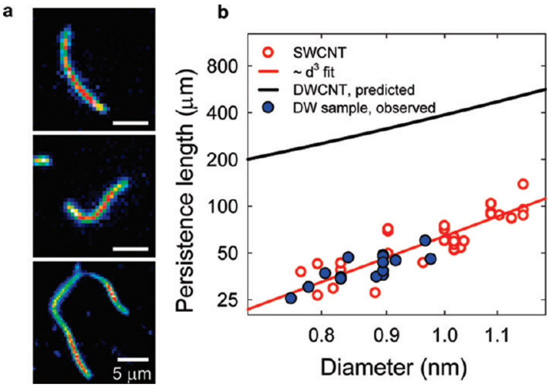

Figure 4. Persistence lengths of individual emissive nanotubes in DWCNT and SWCNT samples. (a) Near-IR fluorescence images of "long" emissive nanotubes in a DWCNT suspension reveal noticeable bending. (b) Persistence lengths measured for individual emissive nanotubes in samples of SWCNTs (open circles, from ref 28) and DWCNTs (solid circles), plotted vs spectroscopically deduced diameter, d. The lower solid line represents the d^3 dependence found for SWCNTs; the upper line shows values predicted for DWCNTs with corresponding inner shell diameters.

SWCNTs in aqueous surfactant suspension, we have found persistence lengths between 30 and 100 μm for SWCNTs with diameters between 0.77 and 1.15 nm and confirmed the theoretical expectation that L_p varies as the cube of nanotube diameter.[28] Because the bending stiffness of a bundle of elastic rods is the sum of its components' χ values, the persistence length of a DWCNT ($L_{\mathrm{P}}^{\mathrm{DW}}$) can be estimated by adding its inner and outer shell persistence lengths. DWCNT outer shells have diameters at least ~0.66 nm greater than the inner shell. This implies that the persistence lengths of DWCNTs with inner shell diameters of 0.7−1.2 nm should exceed those of SWCNTs with the same diameters by factors of approximately 5−9. Thus, bending measurements on long emissive nanotubes in DWCNT suspensions should clearly reveal whether the emitters have single- or double-walled structures.

We captured near-IR fluorescence spectra and image sequences of 17 randomly selected long nanotubes from DWCNT samples in aqueous suspension. Three of these images are displayed in Figure 4a. The solid symbols in Figure 4b show measured persistence lengths of the 17 DWCNT emitters as a function of spectroscopically deduced diameter. Also plotted on this graph (as open symbols) are L_p measurements of nanotubes in a SWCNT sample and two smooth curves representing the d^3 dependence of the SWCNT data and the much higher L_p values predicted for DWCNTs. The persistence lengths found for the emitters in the DWCNT sample are in excellent agreement with those of SWCNTs and fall far below the values expected for DWCNTs.

Our final approach to identifying the source of near-IR emission from DWCNT samples was purification by density gradient ultracentrifugation. This is a bulk method that can sort SWCNTs based on the structure dependence of their buoyant densities in surfactant suspensions.[40] Calculations and a recent experimental report show that density gradient ultracentrifugation can be effective in separating SWCNTs from DWCNTs.[19] We performed density gradient ultracentrifugation on a stock DWCNT suspension and then collected fractions at various depths corresponding to different densities. Figure 5a shows a photo of the centrifuged sample along with a scale identifying the fraction numbers. We analyzed fractions 1−16 by absorption spectroscopy, fluorescence spectroscopy, and HRTEM. The topmost fractions 1−4 (corresponding to densities of 1.046, 1.049, 1.053, and 1.057 g/cm^3, see Supporting Information) had distinct pink, green, and yellow colors. They showed sharp spectral absorption and emission peaks characteristic of SWCNTs with diameters in the range of 0.7−1.0 nm (Figure 5b). These first four fractions accounted for more than 95% of the sample's total near-IR emission. Absorption profiles of fractions 5 to 8 (corresponding to densities of 1.061, 1.066, 1.071, and 1.074 g/cm^3) showed broad peaks near 750 and 1100 nm that shifted to longer wavelengths as the fraction number increased. Because the HRTEM results described below revealed an absence of DWCNTs in these fractions, the features are assigned to E_{11} transitions of metallic SWCNTs and E_{22} transitions of semiconducting SWCNTs with significantly larger diameters (e.g., ~1.75 nm for fraction 7). Some near-IR fluorescence was detectable from each of these collected fractions. In Figure 5d, we plot the emission intensity at 966 nm (a distinct and intense spectral feature of (8,3) nanotubes) and the fractions' absorption at 966 nm as a function of depth in the centrifuged sample tube. The fluorescence signal peaks strongly at fraction 2 (in a low density region near 27 mm) whereas the absorption reaches a peak near fraction 9 in a higher density region. This indicates that the (8,3) emitting species are physically separable from the major absorbers in the sample. As can be deduced from the spectra in Figure 5b, qualitatively similar results were found for other small diameter (n,m) species.

The tail seen in the fluorescence profile suggests cross contamination between fractions, possibly arising from mixing of layers during collection. We therefore repeated the density gradient centrifugation procedure on combined fractions 7−10 (filled circles in Figure 5d), which had very strong absorption and weak emission. Figure 5c shows a photo of this recentrifuged sample. Fluorescence and absorption data were then measured on recentrifuged fractions to give the results plotted in Figure 5e. It can be seen that the residual emissive component in these fractions became separated more completely from the strongly absorbing component, with ~80% of the emission arising from the top 6 fractions. From the data we estimate that the fluorescence/absorption ratio for combined fractions 7 to 10 in Figure 5a is at least a factor of 10 000 lower than for fraction 2. These results suggest that the early, emissive fractions of lower density contain SWCNT impurities from the original DWCNT sample, whereas the later, nonemissive fractions of higher density contain the pure DWCNTs.

To check this interpretation, we analyzed the compositions of density gradient fractions using HRTEM. Figure 6 shows representative images from the multiple frames that were

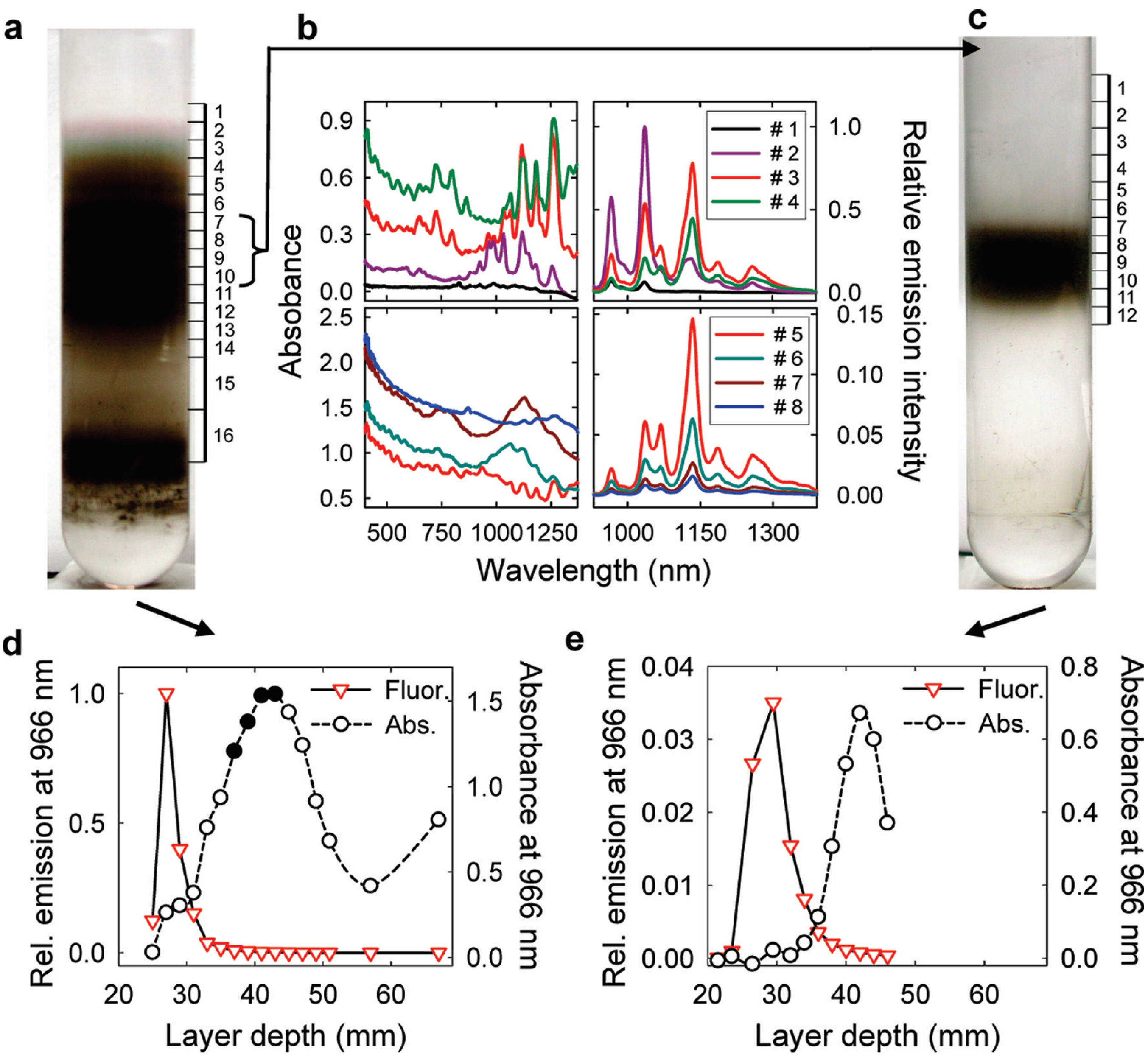

Figure 5. Spectroscopic analysis of density gradient fractionated DWCNT samples. (a) Image of the DWCNT suspension after density gradient centrifugation, showing numbering of the collected fractions. (b) Absorption and fluorescence spectra (excited at 660 nm) of fractions 1−8 collected from the tube shown in panel a. (c) Image of a sample containing fractions 7−10 from the first separation after a second step of density gradient centrifugation. (d) Absorbance (circles) and relative emission intensity (triangles), measured at 966 nm, of fractions from the first separation step. (e) Absorbance (circles) and relative emission intensity (triangles), measured at 966 nm, of fractions collected from the tube shown in panel c after second step processing of fractions 7−10 (marked as solid circles in (d)) from the first separation step.

recorded and analyzed for each fraction. In fractions 1−4 we found only SWCNTs, with typical diameters progressively increasing from approximately 0.7 nm in fraction 1 to 1.0 nm in fraction 4. These findings are consistent with the spectrofluorimetric data in Figure 5b. Fractions 5−7 showed SWCNTs with larger diameters ranging from 1.0−1.6 nm. DWCNTs were not detected in these first seven fractions, but were observed as a small proportion of the nanotubes in fraction 8. The DWCNTs seen in HRTEM images of fractions 8 and 9 have outer and inner shell diameters of ∼1.35 ± 0.1 and 0.6 ± 0.1 nm, respectively. However, significant emission at wavelengths corresponding to such inner shell diameters was detected only from fractions earlier than these. We found that DWCNT abundance and DWCNT diameters increase further in the later, higher density fractions. These later fractions also contain some SWCNTs with very large diameters. Similar HRTEM and spectral results from density gradient fractionation of a smaller diameter DWCNT sample (outer diameters 1.5−2.0 nm) are presented in Supporting Information. HRTEM analysis thus confirmed that density gradient centrifugation of DWCNT samples separates small diameter residual SWCNTs from DWCNTs with comparable inner-tube diameters. Our combined spectrometric and HRTEM measure-

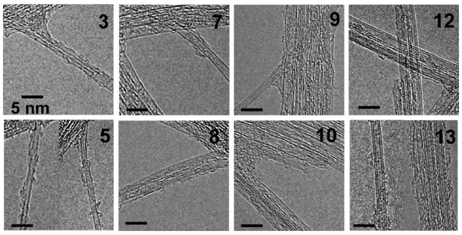

Figure 6. HRTEM images of density gradient fractionated DWCNT samples. The number in the upper right-hand corner of each frame indicates the fraction number as collected from the tube shown in Figure 5a. Fractions 1−7 show exclusively SWCNTs; fractions 10−14 show predominantly DWCNTs.

ments on purified fractions provide evidence that the quantum yield of near-IR emission from DWCNT inner shells is at least 10 000 times lower than for SWCNTs of comparable diameter. We note that Green and Hersam recently reported a milder suppression of fluorescence from DWCNT suspensions purified by density gradient treatment and similarly deduced that the emission of their DWCNT samples came from SWCNT impurities rather than from DWCNT inner shells.[19]

In summary, we have applied a set of complementary experimental methods to clarify the source of near-IR fluorescence from samples of directly grown DWCNTs. Several previous reports have attributed this emission to DWCNT inner shells. Our fluorimetry of bulk DWCNT samples shows emission that is weaker than but spectrally very similar to emission from similarly processed SWCNTs. Measurements on individual nanotubes reveal that the DWCNT sample contains a low relative concentration of emitters that individually match SWCNTs in spectral position, spectral width, and absolute fluorimetric brightness per carbon atom. We find that near-IR fluorescence from DWCNT bulk samples is quickly and efficiently quenched by addition of a reactant that chemically derivatizes nanotube side walls. In this process, individual emitters from the DWCNT sample show stepwise fluorescence quenching from single-molecule reactions that is qualitatively and quantitatively similar to quenching found previously for SWCNTs. All of these findings are consistent with near-IR emission from SWCNT impurities rather than from DWCNT inner shells.

This interpretation is supported by measurements of thermally induced bending amplitudes in long emissive nanotubes in DWNCT suspensions. Each observed nanotube has a stiffness value characteristic of a SWCNT but far lower than expected for a double-walled structure. Finally, spectroscopic and HRTEM analysis of DWCNT samples processed by density gradient centrifugation shows that fractions with emissive SWCNT impurities can be separated from nearly nonemissive fractions containing DWCNTs. These data allow us to estimate that the fluorescence quantum yield of DWCNT inner shells in our samples is at least 4 orders of magnitude below that of SWCNTs of the same diameter. We found very similar results using samples independently prepared and purified (to >95% DWCNT content) by the M. Endo group.[13]

Our findings contradict previous reports of inner shell emission from DWCNTs,[7,11−17] including some studies on samples purified by procedures expected to suppress fluorescence of any SWCNT impurities. It may be that residual SWCNTs trapped within nanotube bundles can evade chemical reaction during such processing and then be freed as the sample is dispersed into surfactant solution. Alternatively, it seems conceivable that a small fraction of inner shells may be exposed or released from DWCNTs during extensive chemical and physical treatment. Whatever the origin of the emissive SWCNT impurities, our study finds that they are the source of near-IR fluorescence previously attributed to DWCNT inner shells.

Acknowledgment. We thank M. Endo for providing DWCNT samples from his laboratory. This research was supported by the NSF (CHE-0809020), the Welch Foundation (C-0807 and C-1668), Applied NanoFluorescence, LLC, the NSF Center for Biological and Environmental Nanotechnology (EEC-0647452), Unidym Inc., and a Duke University GPNANO fellowship.

Supporting Information Available: DWCNT sample characterization by HRTEM and PL; spectral shift data for DWCNT and purified SWCNT samples; density profiles for DGU separations; spectral and HRTEM analyses of DGU fractions from a DWCNT sample containing smaller diameter nanotubes; spectral analyses of DGU fractions from a DWCNT sample prepared by the Endo laboratory; fluorescence quenching in DWCNT suspensions by acid and potassium permanganate; near-IR fluorescence microscopy of SWCNT and DWCNT aggregates; qualitative observations on DWCNT and SWCNT lengths. This material is available free of charge via the Internet at http://pubs.acs.org.

References

(1) Pfeiffer, R.; Pichler, T.; Kim, Y. A.; Kuzmany, H. Double-Wall Carbon Nanotubes. In *Carbon Nanotubes*; Jorio, A., Dresselhaus, G., Dresselhaus, M. S., Eds.; Springer-Verlag: Berlin, 2008; pp 495−530.
(2) Bandow, S.; Takizawa, M.; Hirahara, K.; Yudasaka, M.; Iijima, S. *Chem. Phys. Lett.* **2001**, *337*, 48–54.
(3) Hutchison, J. L.; Kiselev, N. A.; Krinichnaya, E. P.; Krestinin, A. V.; Loutfy, R. O.; Morawsky, A. P.; Muradyan, V. E.; Obraztsova, E. D.; Sloan, J.; Terekhov, S. V.; Zakharov, D. N. *Carbon* **2001**, *39*, 761–770.
(4) Ren, W. C.; Li, F.; Chen, J. A.; Bai, S.; Cheng, H. M. *Chem. Phys. Lett.* **2002**, *359*, 196–202.
(5) Flahaut, E.; Bacsa, R.; Peigney, A.; Laurent, C. *Chem. Commun.* **2003**, 1442–1443.
(6) Endo, M.; Muramatsu, H.; Hayashi, T.; Kim, Y. A.; Terrones, M.; Dresselhaus, M. S. *Nature* **2005**, *433*, 476.
(7) Kishi, N.; Kikuchi, S.; Ramesh, P.; Sugai, T.; Watanabe, Y.; Shinohara, H. *J. Phys. Chem. B* **2006**, *110*, 24816–24821.
(8) O'Connell, M.; Bachilo, S. M.; Huffman, C. B.; Moore, V.; Strano, M. S.; Haroz, E.; Rialon, K.; Boul, P. J.; Noon, W. H.; Kittrell, C.; Ma, J.; Hauge, R. H.; Weisman, R. B.; Smalley, R. E. *Science* **2002**, *297*, 593–596.
(9) Dukovic, G.; White, B. E.; Zhou, Z. Y.; Wang, F.; Jockusch, S.; Steigerwald, M. L.; Heinz, T. F.; Friesner, R. A.; Turro, N. J.; Brus, L. E. *J. Am. Chem. Soc.* **2004**, *126*, 15269–15276.
(10) Cognet, L.; Tsyboulski, D.; Rocha, J.-D. R.; Doyle, C. D.; Tour, J. M.; Weisman, R. B. *Science* **2007**, *316*, 1465–1468.
(11) Hertel, T.; Hagen, A.; Talalaev, V.; Arnold, K.; Hennrich, F.; Kappes, M.; Rosenthal, S.; McBride, J.; Ulbricht, H.; Flahaut, E. *Nano Lett.* **2005**, *5*, 511–514.

(12) Iakoubovskii, K.; Minami, N.; Kazaoui, S.; Ueno, T.; Miyata, Y.; Yanagi, K.; Kataura, H.; Ohshima, S.; Saito, T. *J. Phys. Chem. B* **2006**, *110*, 17420–17424.

(13) Hayashi, T.; Shimamoto, D.; Kim, Y. A.; Muramatsu, H.; Okino, F.; Touhara, H.; Shimada, T.; Miyauchi, Y.; Maruyama, S.; Terrones, M.; Dresselhaus, M. S.; Endo, M. *ACS Nano* **2008**, *2*, 485–488.

(14) Iakoubovskii, K.; Minami, N.; Ueno, T.; Kazaoui, S.; Kataura, H. *J. Phys. Chem. C* **2008**, *112*, 11194–11198.

(15) Hirori, H.; Matsuda, K.; Kanemitsu, Y. *Phys. Rev. B* **2008**, *78*, 113409-1–113409-4.

(16) Kim, J. H.; Kataoka, M.; Kim, Y. A.; Shimamoto, D.; Muramatsu, H.; Hayashi, T.; Endo, M.; Terrones, M.; Dresselhaus, M. S. *Appl. Phys. Lett.* **2008**, *93*, 223107-1–223107-3.

(17) Shimamoto, D.; Muramatsu, H.; Hayashi, T.; Kim, Y. A.; Endo, M.; Park, J. S.; Saito, R.; Terrones, M.; Dresselhaus, M. S. *Appl. Phys. Lett.* **2009**, *94*, 083106-1–083106-3.

(18) Okazaki, T.; Bandow, S.; Tamura, G.; Fujita, Y.; Iakoubovskii, K.; Kazaoui, S.; Minami, N.; Saito, T.; Suenaga, K.; Iijima, S. *Phys. Rev. B* **2006**, *74*, 153404-1–153404-4.

(19) Green, A. A.; Hersam, M. C. *Nat. Nanotechnol.* **2009**, *4*, 64–70.

(20) Qian, H.; Goergi, C.; Anderson, N.; Green, A. A.; Hersam, M. C.; Novotny, L.; Hartschuh, A. *Nano Lett.* **2008**, *8*, 1363–1367.

(21) Thess, A.; Lee, R.; Nikolaev, P.; Dai, H. J.; Petit, P.; Robert, J.; Xu, C. H.; Lee, Y. H.; Kim, S. G.; Rinzler, A. G.; Colbert, D. T.; Scuseria, G. E.; Tomanek, D.; Fischer, J. E.; Smalley, R. E. *Science* **1996**, *273*, 483–487.

(22) Colomer, J.-F.; Henrard, L.; Lambin, P.; Van Tendeloo, G. *Eur. Phys. J. B* **2002**, *27*, 111–118.

(23) Tsyboulski, D. A.; Bachilo, S. M.; Weisman, R. B. *Nano Lett.* **2005**, *5*, 975–979.

(24) Tsyboulski, D.; Rocha, J.-D. R.; Bachilo, S. M.; Cognet, L.; Weisman, R. B. *Nano Lett.* **2007**, *7*, 3080–3085.

(25) Bahr, J. L.; Yang, J.; Kosynkin, D. V.; Bronikowski, M. J.; Smalley, R. E.; Tour, J. M. *J. Am. Chem. Soc.* **2001**, *123*, 6536–6542.

(26) Bachilo, S. M.; Strano, M. S.; Kittrell, C.; Hauge, R. H.; Smalley, R. E.; Weisman, R. B. *Science* **2002**, *298*, 2361–2366.

(27) Duggal, R.; Pasquali, M. *Phys. Rev. Lett.* **2006**, *96*, 246104-1–246104-4.

(28) Fakhri, N.; Tsyboulski, D. A.; Cognet, L.; Weisman, R. B.; Pasquali, M. *Proc. Natl. Acad. Sci. U.S.A.*, in press, DOI: 10.1073/pnas.0904148106.

(29) Gittes, F.; Mickey, B.; Nettleton, J.; Howard, J. *J. Cell Biol.* **1993**, *120*, 923–934.

(30) Wang, F.; Sfeir, M. Y.; Huang, L.; Huang, X. M. H.; Wu, Y.; Kim, J.; Hone, J.; O'Brien, S.; Brus, L. E.; Heinz, T. F. *Phys. Rev. Lett.* **2006**, *96*, 167401-1–167401-4.

(31) Choi, J. H.; Strano, M. S. *Appl. Phys. Lett.* **2007**, *90*, 223114-1–223114-3.

(32) Ohno, Y.; Iwasaki, S.; Murakami, Y.; Kishimoto, S.; Maruyama, S.; Mizutani, T. *Phys. Status Solidi B* **2007**, *244*, 4002–4005.

(33) Blackburn, J. L.; McDonald, T. J.; Metzger, W. K.; Engtrakul, C.; Rumbles, G.; Heben, M. J. *Nano Lett.* **2008**, *8*, 1047–1054.

(34) Lefebvre, J.; Fraser, J. M.; Finnie, P.; Homma, Y. *Phys. Rev. B* **2004**, *69*, 075403-1−075403-5.

(35) Tsyboulski, D. A.; Bakota, E. L.; Witus, L. S.; Rocha, J. D. R.; Hartgerink, J. D.; Weisman, R. B. *J. Am. Chem. Soc.* **2008**, *130*, 17134–17140.

(36) Strano, M. S.; Dyke, C. A.; Usrey, M. L.; Barone, P. W.; Allen, M. J.; Shan, H.; Kittrell, C.; Hauge, R. H.; Tour, J. M.; Smalley, R. E. *Science* **2003**, *301*, 1519–1522.

(37) Doyle, C. D.; Rocha, J.-D. R.; Weisman, R. B.; Tour, J. M. *J. Am. Chem. Soc.* **2008**, *130*, 6795–6800.

(38) Tsyboulski, D. A.; Bachilo, S. M.; Kolomeisky, A. B.; Weisman, R. B. *ACS Nano* **2008**, *2*, 1770–1776.

(39) Doi, M.; Edwards, S. F. *The Theory of Polymer Dynamics*; Oxford University Press: New York, 1986.

(40) Arnold, M. S.; Green, A. A.; Hulvat, J. F.; Stupp, S. I.; Hersam, M. C. *Nat. Nanotechnol.* **2006**, *1*, 60–65.

NL901550R